Reprinted from the Journal of Applied Mechanics,
Volume 42, Number 1, Pages 183-189, March 1975

J. D. Achenbach
Professor. Mem. ASME

Z. P. Bažant
Professor. Mem. ASME

Department of Civil Engineering,
The Technological Institute,
Northwestern University,
Evanston, Ill.

Elastodynamic Near-Tip Stress and Displacement Fields for Rapidly Propagating Cracks in Orthotropic Materials

The near-tip angular variations of elastodynamic stress and displacement fields are investigated for rapid transient crack propagation in isotropic and orthotropic materials. The two-dimensional near-tip displacement fields are assumed in the general form r^p $T(t, c)$ $K(\theta, c)$, where c is a time-varying velocity of crack propagation, and it is shown that $p = 0.5$. For isotropic materials, $K(\theta, c)$ is determined explicitly by analytical considerations. A numerical procedure is employed to determine $K(\theta, c)$ for orthotropic materials. The tendency of the maximum stresses to move out of the plane of crack propagation as the speed of crack propagation increases is more pronounced for orthotropic materials, for the case that the crack propagates in the direction of the larger elastic modulus. The angular variations of the near-tip fields are the same for steady-state and transient crack propagation, and for propagation along straight and curved paths, provided that the direction of crack propagation and the speed of the crack tip vary continuously.

Introduction

In brittle fracture of elastic solids, cracks can propagate at velocities large enough, so that the fields of stress and deformation are significantly influenced by elastodynamic effects. One particularly noteworthy feature of elastodynamic stress fields near a propagating crack tip is that the maximum values of the stresses move out of the plane of crack propagation when the speed of the crack tip exceeds a certain critical value. This feature was first observed by Yoffe [1],[1] and it is also shown in the work of Craggs [2] and Baker [3].

The evaluation of complete and explicit expressions for elastodynamic stress-intensity factors requires the solution of complicated mixed boundary-value problems. Mathematical methods for the analysis of elastodynamic stress fields near propagating cracks have been discussed in reference [4]. The objective of the present paper is to study the nature of the near-tip fields by using a technique which was introduced in static elasticity by Knein [5] and Williams [6].

The Knein-Williams technique has previously been applied to steady-state elastodynamic crack propagation by Cotterell [7], who has not, however, obtained the proper solutions. For steady-state elastodynamic problems the general nature of near-tip stress fields in isotropic materials was analyzed by Rice [8] by means of an analysis based on complex-variable techniques. This type of approach was used by Freund and Clifton [9] for the analysis of the near-tip fields for nonuniform crack propagation in isotropic materials. In a recent note, Nilsson [10] has also examined the angle-dependence of the near-tip fields in isotropic materials.

Analytical Approach

Fig. 1 shows a two-dimensional crack which propagates along a rather arbitrary but smooth trajectory. At time $t = t_1$ the crack is located at point 0_1; at time $t = t_1 + \Delta t$ the crack tip is located at point 0_2. A system of moving Cartesian coordinates x and y is centered at the crack tip, such that the x-axis is along the tangent to the trajectory. In addition, a system of moving polar coordinates (r, θ) is introduced as shown in Fig. 1. The velocity of the crack tip along the trajectory is $c(t)$, where $c(t)$ is an arbitrary function of time, subject to the conditions that $c(t)$ and $\dot{c}(t)$ are continuous

[1] Numbers in brackets designate References at end of paper.

Contributed by the Applied Mechanics Division and presented at the Applied Mechanics Western Conference, University of Hawaii, Honolulu, Hawaii, March 25–27, 1975, of THE AMERICAN SOCIETY OF MECHANICAL ENGINEERS.

Discussion on this paper should be addressed to the Editorial Department, ASME, United Engineering Center, 345 East 47th Street, New York, N. Y. 10017, and will be accepted until May 15, 1975. Discussion received after this date will be returned. Manuscript received by ASME Applied Mechanics Division, October, 1974; final revision, December, 1974. Paper No. 75-APMW-42.

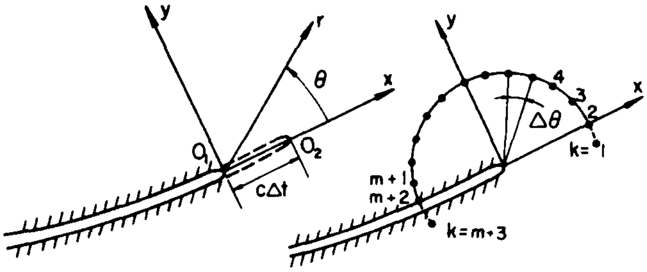

Fig. 1 Propagation of a two-dimensional crack along a smooth trajectory

and bounded. Furthermore, $0 < c(t) < c_T$ and $0 < c(t) < c_R$, for antiplane and in-plane motions, respectively, where c_T is the velocity of transverse waves and c_R is the velocity of Rayleigh waves. As the crack propagates, the x-axis rotates counterclockwise at an angular velocity $R(t)$. It is assumed that $R(t)$ and $\dot{R}(t)$ are bounded continuous functions of time.

In a plane two-dimensional geometry, the system of displacement equations of motion governing linearized elasticity splits into two uncoupled systems, for in-plane and antiplane displacements, respectively; see, e.g., reference [11].

Antiplane Motions. We will first consider crack propagation in antiplane strain. For engineering materials this case has limited physical significance, since under antiplane loading, materials generally appear to fracture in a more complicated fashion, except perhaps in geophysical settings with preexisting fracture planes. A brief discussion of the antiplane strain case serves, however, the very useful purpose of establishing the general ideas and of presenting the method of analysis, which will then subsequently be used for the case of in-plane motions.

Let the antiplane displacement be instantaneously defined in terms of the moving coordinate system (x, y); i.e., $w = w(x, y, t)$. The material derivative with respect to time, which is indicated by a superimposed dot, is then of the form

$$\dot{w} = \frac{\partial w}{\partial t} - c(t)\frac{\partial w}{\partial x} - R(t)\left(x\frac{\partial w}{\partial y} - y\frac{\partial w}{\partial x}\right) \tag{1}$$

It follows from equation (1) that

$$\begin{aligned}\ddot{w} = {} & c^2\frac{\partial^2 w}{\partial x^2} - \dot{c}\frac{\partial w}{\partial x} - 2c\frac{\partial^2 w}{\partial t\partial x} + \frac{\partial^2 w}{\partial t^2} \\ & - Rx\left[\frac{\partial^2 w}{\partial t\partial y} - (c - Ry)\frac{\partial^2 w}{\partial x\partial y} + R\frac{\partial w}{\partial x} - Rx\frac{\partial^2 w}{\partial y^2}\right] \\ & + Ry\left[\frac{\partial^2 w}{\partial t\partial x} - (c - Ry)\frac{\partial^2 w}{\partial x^2} - R\frac{\partial w}{\partial y} - Rx\frac{\partial^2 w}{\partial x\partial y}\right] \\ & - \dot{R}\left(x\frac{\partial w}{\partial y} - y\frac{\partial w}{\partial x}\right) - R\left(x\frac{\partial^2 w}{\partial t\partial y} - y\frac{\partial^2 w}{\partial t\partial x}\right) \\ & + cR\frac{\partial}{\partial x}\left(x\frac{\partial w}{\partial y} - y\frac{\partial w}{\partial x}\right)\end{aligned} \tag{2}$$

Relative to the moving system of Cartesian coordinates the displacement equation of motion is

$$\frac{\partial^2 w}{\partial x^2} + \frac{\partial^2 w}{\partial y^2} = \frac{1}{c_T^2}\ddot{w}. \tag{3}$$

Following an idea introduced in static elasticity by Knein [5] and Williams [6] we seek the displacement in the immediate vicinity of the moving crack tip in the general form

$$w(r,\theta,t) = C\, r^q T(t) W(\beta,\theta), \tag{4}$$

where C is an arbitrary constant, and β is defined by

$$\beta = c(t)/c_T \tag{5}$$

The conditions of vanishing stress on the crack surfaces and of antisymmetry of the displacement field require that

$$\text{At } \theta = \pm\pi:\ \partial W/\partial\theta = 0; \quad \text{At } \theta = 0:\ W = 0 \tag{6a,b}$$

respectively. The exponent q and the function $W(\beta, \theta)$ are considered as yet unknown.

Substituting equation (4) into equation (3), with $\ddot{w}$ according to (2), multiplying the result by r^{2-q}, and considering the limit $r \to 0$, the following equation is obtained:

$$\begin{aligned}(1 - \beta^2\sin^2\theta)\frac{d^2W}{d\theta^2} - \beta^2(1 - q)\sin 2\theta\frac{dW}{\partial\theta} \\ + q\{q + \beta^2[(2 - q)\cos^2\theta - 1]\}W = 0\end{aligned} \tag{7}$$

Here it should be noted that only the first term of $\ddot{w}$, equation (2), contributes to equation (8). The other terms are of the types $F_1(t)r$ and $F_2(t)r^2$, where $F_1(t)$ and $F_2(t)$ are lengthy linear combinations of products of W and its derivatives with $c(t)$, $R(t)$, and $T(t)$ and their derivatives and with various trigonometric functions of θ. In the limit $r \to 0$ the terms $F_1(t)r$ and $F_2(t)r^2$ vanish, provided $\dot{c}$, $\dot{R}$, and $\dot{T}$ are bounded. This proves that the angular variations of the near-tip fields must be the same for steady and transient crack propagation, and for straight and curved crack tip trajectories.

Let us seek a solution of equation (7) in the form

$$W(\beta,\theta) = (1 - \beta^2\sin^2\theta)^{q/2}W^*(\beta,\theta) \tag{8}$$

Substitution of equation (8) into equation (7) yields a much simpler equation for W^*, which can, however, be further simplified by introducing the variable ω by[2]

$$\tan\omega = (1 - \beta^2)^{1/2}\tan\theta \tag{9}$$

The resulting equation for $W^*(\beta, \omega)$ is

$$\frac{d^2W^*}{d\omega^2} + q^2W^* = 0 \tag{10}$$

In view of the boundary condition at $\theta = 0$, (see equation (6b)), the appropriate solution of equation (10) is

$$W^*(\beta,\omega) = A\sin q\omega \tag{11}$$

The boundary condition at $\theta = \pi$, equation (6a) gives $dW^*/d\omega = 0$ at $\theta = \pi$, or $\cos q\pi = 0$, which yields as the lowest root

$$q = \frac{1}{2} \tag{12}$$

An expression for $W(\beta, \omega)$ follows from equations (8) and (11). Upon subsequent elimination of ω in favor of θ by means of equation (9), we find

$$W(\beta,\theta) = [(1 - \beta^2\sin^2\theta)^{1/2} - \cos\theta]^{1/2}\frac{A}{\sqrt{2}} \tag{13}$$

An alternative expression for $W(\beta, \theta)$ which results when $\sin(1/2)\omega$ in equation (17) is expressed as $\sin(\omega - (1/2)\omega)$ is as follows:

$$W(\beta,\theta) = [\Psi_1\cos\theta - (1 - \beta^2)^{1/2}\Psi_2\sin\theta]\frac{A}{\sqrt{2}} \tag{14}$$

where Ψ_1 and Ψ_2 are defined by

---

[2] Substitutions (8) and (9) are suggested by noting that the Lorentz transformation $\xi = x/(1 - \beta^2)^{1/2}$, $\eta = y$ reduces equation (3) for $r \to 0$ to Laplace equation $\partial^2w/\partial\xi^2 + \partial^2w/\partial\eta^2 = 0$. It is then natural to introduce new coordinates ρ and ω which are polar coordinates relative to ξ and η, i.e., $\xi = \rho\cos\omega$, $\eta = \rho\sin\omega$. Eliminating ξ and η from the preceding coordinate transformations, one gets equation (9) and the relation $r = (1 - \beta^2)^{1/2}\rho(1 - \beta^2\sin^2\theta)^{-1/2}$ whose substitution into equation (4) leads to equation (8).

$$\Psi_1 = \left[\frac{(1-\beta^2\sin^2\theta)^{1/2} - \cos\theta}{1-\beta^2\sin^2\theta}\right]^{1/2},$$

$$\Psi_2 = \left[\frac{(1-\beta^2\sin^2\theta)^{1/2} + \cos\theta}{1-\beta^2\sin^2\theta}\right]^{1/2} \quad (15a,b)$$

In-Plane Motions. It is convenient to employ displacement potentials φ and ψ, defined by the relations $u = \partial\varphi/\partial x + \partial\psi/\partial y$, $v = \partial\varphi/\partial y - \partial\psi/\partial x$, where φ and ψ are solutions of

$$\frac{\partial^2\varphi}{\partial x^2} + \frac{\partial^2\varphi}{\partial y^2} = \frac{1}{\kappa^2 c_T^2}\ddot{\varphi};\ \frac{\partial^2\psi}{\partial x^2} + \frac{\partial^2\psi}{\partial y^2} = \frac{1}{c_T^2}\ddot{\psi}, \quad (16a,b)$$

where $\kappa^2 = c_L^2/c_T^2 = 2(1-\nu)/(1-2\nu)$, ν being the Poisson's ratio, $c_L^2 = (\lambda + 2\mu)/\rho$, and $\ddot{\varphi}$ and $\ddot{\psi}$ are defined analogously to equation (2).

In the vicinity of the crack tip, expressions for the potentials φ and ψ are sought in the forms

$$\varphi(r,\theta,t) = r^p T(t)\Phi(\alpha,\theta),\ \psi(r,\theta,t) = r^p T(t)\Psi(\beta,\theta) \quad (17a,b)$$

respectively, where

$$\alpha = \frac{c(t)}{c_L} = \frac{c(t)}{\kappa c_T} = \frac{\beta}{\kappa} \quad (18)$$

In order that the strain energy density be integrable, we must have Re $(p) > 1$. In the system of polar coordinates the boundary conditions on the surface of the propagating crack are $\tau_\theta = 0$ and $\tau_{r\theta} = 0$, for $\theta = \pm\pi$, $r > 0$, which yields at $\theta = \pm\pi$

$$(\beta^2 - 2)p\Phi - 2\frac{d\Psi}{d\theta} = 0,\quad 2\frac{d\Phi}{d\theta} + (\beta^2 - 2)p\Psi = 0 \quad (19a,b)$$

For Mode I fracture the displacements are symmetric with respect to $y = 0$, and thus $\partial u/\partial\theta = 0$ and $v = 0$, for $\theta = 0$, $r > 0$, while for Mode II fracture the displacement field is antisymmetric with respect to $y = 0$, which implies $\partial v/\partial\theta = 0$ and $u = 0$, for $\theta = 0$, $r > 0$. These conditions yield

$$\text{For Mode I},\ \theta = 0:\ d\Phi/d\theta = 0,\ \Psi = 0 \quad (20)$$

$$\text{For Mode II},\ \theta = 0:\ \Phi = 0,\ d\Psi/d\theta = 0 \quad (21)$$

The method of solution for $\Phi(\alpha, \theta)$ and $\Psi(\beta, \theta)$ is completely analogous to the method used for solving $W(\beta, \theta)$. Analogously to the development following equation (7) the pertinent solutions satisfying the boundary conditions (20) for the *symmetric problem* may then be written as

$$\Phi(\alpha,\theta) = (1 - \alpha^2\sin^2\theta)^{p/2}A\cos(p\epsilon) \quad (22)$$

$$\Psi(\beta,\theta) = (1 - \beta^2\sin^2\theta)^{p/2}B\sin(p\omega) \quad (23)$$

where ω is defined by equation (9), and in an analogous manner, ϵ is defined by

$$\tan\epsilon = (1-\alpha^2)^{1/2}\tan\theta \quad (24)$$

Substituting equations (22) and (23) into the boundary conditions (19a,b) yields two homogeneous equations for the constants A and B. The requirement that the determinant of the coefficients must vanish as the condition for existence of a solution, yields

$$D(\beta,\alpha)\sin(p\pi)\cos(p\pi) = 0, \quad (25)$$

where $D(\beta, \alpha)$ is the well-known Rayleigh function

$$D(\beta,\alpha) = (\beta^2 - 2)^2 - 4(1-\beta^2)^{1/2}(1-\alpha^2)^{1/2} \quad (26)$$

For a velocity of crack propagation smaller than the Rayleigh wave velocity, the smallest root p of equation (25) for which Re (p) is smallest and greater than unity is $p = 3/2$. From equation (19b) it follows that $A = (\beta^2 - 2)B/2(1-\alpha^2)^{1/2}$. Substitution of the result $p = 3/2$ into equation (22) yields after some trigonometric manipulation, and after expressing $\cos(3\epsilon/2)$ as $\cos(2\epsilon - \epsilon/2)$,

$$\Phi(\alpha,\theta) = \left\{(1-\alpha^2)^{1/2}\Phi_1\sin 2\theta + \left[\left(1 - \frac{\alpha^2}{2}\right)\cos 2\theta + \frac{\alpha^2}{2}\right]\Phi_2\right\}\frac{A}{\sqrt{2}} \quad (27)$$

where

$$\Phi_1 = \left[\frac{(1-\alpha^2\sin\theta)^{1/2} - \cos\theta}{1-\alpha^2\sin^2\theta}\right]^{1/2},$$

$$\Phi_2 = \left[\frac{(1-\alpha^2\sin^2\theta)^{1/2} + \cos\theta}{1-\alpha^2\sin^2\theta}\right]^{1/2} \quad (28a,b)$$

In the same manner we find from equation (23)

$$\Psi(\beta,\theta) = \left\{-\left[\left(1 - \frac{\beta^2}{2}\right)\cos 2\theta + \frac{\beta^2}{2}\right]\Psi_1 + (1-\beta^2)^{1/2}\Psi_2\sin 2\theta\right\}\frac{B}{\sqrt{2}} \quad (29)$$

Here Ψ_1 and Ψ_2 are defined by equations (15a,b).

The functions Φ and Ψ governing the dependence on the angle θ of the potentials for the *antisymmetric* problem (Mode II fracture) follow from the boundary conditions (21) and (19a,b) as

$$\Phi(\alpha,\theta) = (1-\alpha^2\sin^2\theta)^{3/2}A\sin(3\epsilon/2) \quad (30)$$

$$\Psi(\beta,\theta) = (1-\beta^2\sin^2\theta)^{3/2}B\cos(3\omega/2) \quad (31)$$

where $A = (1-\beta^2)^{1/2}B/(1-\beta^2/2)$. It is evident now that Φ is of the form given by equation (29) with β replaced by α, and Ψ is of the form (27), with α replaced by β. The relevant stresses in the system of polar coordinates, r, θ, follow from Hooke's law.

It has been checked that the limits for $c \to 0$ yield the well-known expressions for the near-tip fields for stationary cracks, listed in reference [12]. It can further be shown that the results of this section apply directly to a crack of rather arbitrarily curved front propagating in its own plane in an isotropic material, provided that the radius of curvature of the crack front varies smoothly, and that at any instant the speed of crack propagation in the normal direction is uniform along the entire crack front.

Displacement Formulation for Orthotropic Materials

For crack propagation in an anisotropic material, it appears to be necessary to analyze the near-tip fields by means of a numerical method, based on a displacement formulation.

In-Plane Motions. The stress-strain relations for an orthotropic material are

$$\tau_x = E_{xx}\frac{\partial u}{\partial x} + E_{xy}\frac{\partial v}{\partial y};$$

$$\tau_y = E_{yx}\frac{\partial u}{\partial x} + E_{yy}\frac{\partial v}{\partial y};\ \tau_{xy} = G_{xy}\left(\frac{\partial u}{\partial y} + \frac{\partial v}{\partial x}\right) \quad (32a,b,c)$$

The x and y-axes coincide with the axes of material orthotropy; G_{xy}, E_{xx}, E_{yy} and $E_{xy} = E_{yx}$ are four independent elastic moduli. For an *isotropic* material we have $G_{xy} = \mu$; $E_{xx} = E_{yy} = 2\mu(1-\nu)/(1-2\nu)$; $E_{xy} = E_{yx} = 2\mu\nu/(1-2\nu)$.

We will consider a crack propagating at velocity $c(t)$ in the x-direction, which is an axis of material orthotropy. Relative to coordinates x and y moving with the crack tip, a set of displacement equations of motion is obtained by substituting equations (32a,b,c) in the stress equations of motion, and expressing the acceleration terms $\ddot{u}$ and $\ddot{v}$ in the manner indicated by equation (2). We obtain

$$(E_{xx} - G_{xy}\beta^2)\frac{\partial^2 u}{\partial x^2} + (E_{xy} + G_{xy})\frac{\partial^2 v}{\partial x\partial y} + G_{xy}\frac{\partial^2 u}{\partial y^2} = 0 \quad (33)$$

$$G_{xy}(1-\beta^2)\frac{\partial^2 v}{\partial x^2} + (E_{xy} + G_{xy})\frac{\partial^2 u}{\partial x\partial y} + E_{yy}\frac{\partial^2 v}{\partial y^2} = 0 \quad (34)$$

where $\beta = c(t)/(c_T)_{xy}$, $(c_T)_{xy} = (G_{xy}/\rho_0)^{1/2}$. Here ρ_0 is the mass density. Only the first term of the expressions for $\ddot{u}$ and $\ddot{v}$ of the type of equation (2) has been considered in equations (33) and (34), because all remaining terms are negligible for $r \to 0$, similarly as in equation (7). Equations (33) and (34) may now be transformed to polar coordinates r, θ. Similarly to the previous section, the Cartesian displacement components near the crack tip are subsequently sought in the forms

$$u = r^q U(\theta)T(t), \quad v = r^q V(\theta)T(t) \tag{35a,b}$$

Substituting these expressions into equations (33) and (34) after their transformation to polar coordinates, multiplying the result by r^{2-q}, and considering the limit $r \to 0$, we obtain

$$\begin{aligned}[][(E_{xx} - \beta^2 G_{xy}) \sin^2\theta + G_{xy}\cos^2\theta]\frac{d^2U}{d\theta^2} + (E_{xx} - \beta^2 G_{xy} \\ - G_{xy})(1-q)\sin 2\theta \frac{dU}{d\theta} + q\{[G_{xy} - (1-q)(E_{xx} \\ - \beta^2 G_{xy})]\cos^2\theta + [E_{xx} - (\beta^2 + 1 - q)G_{xy}]\sin^2\theta\}U \\ - (E_{xy} + G_{xy})\left\{\frac{\sin 2\theta}{2}\frac{d^2V}{d\theta^2} + (1-q)\cos 2\theta\frac{dV}{d\theta} \right. \\ \left. + q(2-q)\frac{\sin 2\theta}{2}V\right\} = 0\end{aligned} \tag{36}$$

$$\begin{aligned}[][(1-\beta^2)G_{xy}\sin^2\theta + E_{yy}\cos^2\theta]\frac{d^2V}{d\theta^2} + [(1-\beta^2)G_{xy} \\ - E_{yy}](1-q)\sin 2\theta\frac{dV}{d\theta} + q\{[E_{yy} - (1-q)(1 \\ - \beta^2)G_{xy}]\cos^2\theta + [(1-\beta^2)G_{xy} - (1-q)E_{yy}]\sin^2\theta\}V \\ - (E_{xy} + G_{xy})\left\{\frac{\sin 2\theta}{2}\frac{d^2U}{d\theta^2} + (1-q)\cos 2\theta\frac{dU}{d\theta}\right. \\ \left. + q(2-q)\frac{\sin 2\theta}{2}U\right\} = 0\end{aligned} \tag{37}$$

The boundary conditions $\tau_y = 0$ and $\tau_{xy} = 0$ on the surface of the crack yield

$$\text{At } \theta = \pm\pi: \quad \frac{dU}{d\theta} = -qV, \quad \frac{dV}{d\theta} = -\frac{E_{xy}}{E_{yy}}qU \tag{38}$$

The Mode I crack is characterized by the conditions of symmetry

$$\text{At } \theta = 0: \quad \frac{dU}{d\theta} = 0, \quad V = 0 \text{ (Mode I)} \tag{39}$$

and the Mode II crack is characterized by the conditions of antisymmetry

$$\text{At } \theta = 0: \quad U = 0, \quad \frac{dV}{d\theta} = 0 \text{ (Mode II)} \tag{40}$$

Having solved for the functions U and V, the stresses may be obtained from equations (32a,b,c) with strains expressed in terms of u and v, converting the derivatives to polar coordinates, and substituting equations (35a,b).

Antiplane Motions. Introducing new variables $\bar{x} = x$, $\bar{y} = (G_{xz}/G_{yz})\, y$, the antiplane equation of motion becomes formally identical with equation (3). Thus it can be shown that the near-tip fields for the case of orthotropic material can be immediately obtained from equation (4), and (13)–(15), merely by the following replacements:

$$\theta \longrightarrow \arctan[(G_{xz}/G_{yz})\tan\theta], \quad r \longrightarrow r[\cos^2\theta + (G_{xz}/G_{yz})^2\sin^2\theta]^{1/2} \tag{41}$$

Numerical Method

Equations (36) and (37) with boundary conditions (38)–(40) define an eigenvalue problem for q. By virtue of the one-dimensionality of the system of differential equations, a numerical solution by the finite-difference method is a simple task with the aid of a high-speed computer. By means of the numerical solution we not only verify the well-known result that $q = 0.5$ for a crack propagating in a homogeneous medium, but we also obtain U and V as functions of θ for chosen values of β.

In the numerical computations the interval $\theta \in (0, \pi)$ is subdivided by $(m + 1)$ nodes into m equal subintervals $\Delta\theta$, and one exterior node is introduced a distance $\Delta\theta$ from each end in order to formulate the boundary conditions; see Fig. 1(*b*). The derivatives in equations (36)–(40) are approximated by the well-known second-order finite-difference formulas, e.g.,

$$\left(\frac{dU}{d\theta}\right)_k \approx \frac{U_{k+1} - U_{k-1}}{2\Delta\theta}, \quad \left(\frac{d^2U}{d\theta^2}\right)_k \approx \frac{U_{k+1} - 2U_k + U_{k-1}}{\Delta\theta^2}, \ldots \tag{42}$$

where subscript k refers to the node number. In this manner one obtains a system of linear algebraic equations

$$\sum_{j=1}^{N} A_{ij}(q)X_j = 0 \quad (i = 1, 2, \ldots N), \tag{43}$$

where $X_{2k-1} = U_k$, $X_{2k} = V_k$, $N = 2(m + 3)$. To assemble the matrix A_{ij} for a given q, one evaluates for each node k the coefficients of the differential equations (36) and (37), denoted as C_{rsd}, where $r = 1$ for equation (36), and $r = 2$ for equation (37); $s = 1$ or 2 for the coefficient of U or its derivatives, or of V or its derivatives, respectively; d refers to the order of derivative of U or V: $d = 3$ for a second derivative, $d = 2$ for a first derivative, and $d = 1$ for no derivative. For $k = 1$ and $k = m + 3$, C_{rsd} are used to denote the coefficients in the boundary conditions (38)–(40). Subsequently, the finite-difference forms of the differential equations (36) and (37) for the kth node are considered in the form

$$c_{r11}U_{k-1} + c_{r12}U_k + c_{r13}U_{k+1} + c_{r21}V_{k-1} + c_{r22}V_k + c_{r23}V_{k+1} = 0 \quad (r = 1, 2) \tag{44}$$

The coefficients are evaluated as

$$c_{rs1} = \frac{1}{\Delta\theta^2}C_{rs3} - \frac{1}{2\Delta\theta}C_{rs2}, \; c_{rs2} = C_{rs1} - \frac{2}{\Delta\theta^2}C_{rs3}, \; c_{rs3} = \frac{1}{\Delta\theta^2}C_{rs3} + \frac{1}{2\Delta\theta}C_{rs2} \tag{45}$$

$$(r = 1, 2; \; s = 1, 2)$$

Matrix A_{ij} may then be assembled from coefficients c_{rsn} for all nodes $k = 1, \ldots N$ according to the relations $A_{ij} = C_{rs2}$, $A_{i\,j-2} = C_{rs1}$, $A_{i\,j+2} = C_{rs3}$, where $i = 2k - 2 + r$, $j = 2k - 2 + s$. In practice, one of course takes advantage of the fact that matrix A_{ij} is banded, with bandwidth 7, and stores the band of matrix A_{ij} in a rectangular ($N \times 7$) matrix A'_{il} whose elements are for each k determined as $A'_{il} = A_{ij}$ where $l = j - i + 4$.

A FORTRAN IV program was written to assemble and solve equation (43). A subdivision of the interval $(0, \pi)$ into 96 subintervals was used, which resulted in a system of 198 equations for the in-plane case and 99 equations for the antiplane case. First, it was checked that $q = 0.5$ is indeed the smallest eigenvalue. For this purpose, an efficient method of searching for the roots of equation (43), developed and extensively tested in reference [13] and also applied in reference [14], was utilized. The search for the smallest root yielded the value $q = 0.4998$ for the case of Mode III fracture in an isotropic material, at $\beta^2 = 0.5$, and the value $q = 0.5003$ for the case of Mode I fracture. These results indicate a very high accuracy of the numerical solution. Similar accuracy was achieved for other β and for the orthotropic material.

In general, there are two eigenstates associated with root $q = 0.5$ in the plane case, one symmetric and one antisymmetric. Thus, if symmetry or antisymmetry boundary conditions (39) or (40) are specified, one is certain that the equation system (43) must become nonsingular by replacing one equation, the nth equation, with the equation $X_n = 1$, provided that c is less than the Rayleigh wave speed. The same is true of the antiplane motion, provided c

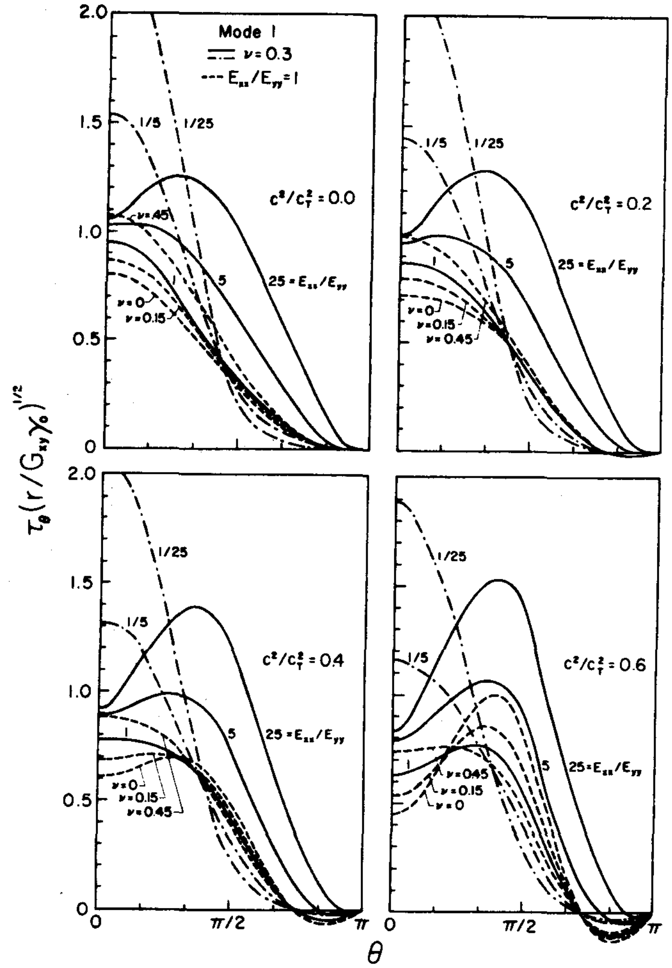

Fig. 2 Angular variation of τ_θ for Mode I fracture. (Solid lines are for $E_{xx} \geq E_{yy}$, dash-dot lines for $E_{xx} < E_{yy}$, all for $\nu = 0.3$. The dashed lines are for various ν, all for $E_{xx} = E_{yy}$. The values of G_{xy}/E and E_{xy}/E equal those for an isotropic material of Poisson ratio ν, E being the smaller of E_{xx} and E_{yy}; i.e., $G_{xy}/E = (0.5 - \nu)/(1 - \nu)$, $E_{xy}/E = \nu/(1 - \nu)$).

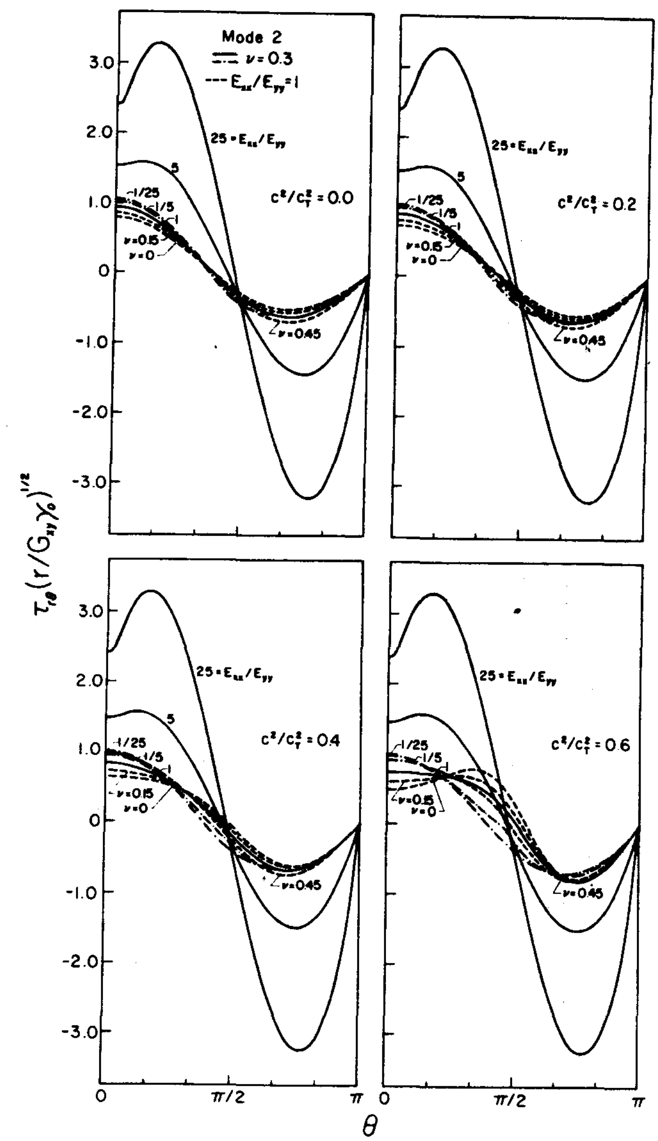

Fig. 3 Angular variations of $\tau_{r\theta}$ for Mode II fracture; see Fig. 2 caption for further explanation

$< c_T$. It is also necessary to choose n in such a manner that X_n is nonzero in the eigenstate to be solved, but barring poor judgement this case does not happen. For good accuracy, however, it is advisable to choose n in such a manner that $|X_n|$ is not much less than $\max |X_i|$ $(i = 1, \ldots N)$. Subsequently, the system of equations is solved for X_i by a standard library subroutine for band matrices. The stresses are then evaluated from formulas in which the derivatives are approximated by finite-difference expressions.

To give an indication of the accuracy, it may be mentioned that for the case of an isotropic material, and a Mode I crack at $\beta^2 = 0.5$, the maximum error in U and V, as compared with the values obtained from the exact solution as presented in an earlier section, was 0.0012 of the maximum value of $|U|$ and 0.0005 of the maximum value of $|V|$, and the mean square errors were 0.0007 and 0.0003 of these values. Similar accuracy was obtained for Mode II and Mode III cracks and for other velocities of crack propagation. The accuracy achieved is satisfactory for all practical purposes.

In the numerical method described, the eigenstate $X_i(\theta)$ is obtained up to an arbitrary multiplier, and it is, therefore, desirable to normalize the eigenstates in a suitable manner. For fracture mechanics considerations it is useful to normalize the eigenstates with respect to one half of the specific energy of crack extension, γ_0, and with respect to the elastic modulus, G_{xy}.

It has been shown in references [4, 15] that the flux of energy into the moving crack tip may be expressed in terms of the stresses and particle velocities in the plane of crack propagation,

$$F = \pi[\tau_y(0)\dot{v}(\pi) + \tau_{xy}(0)\dot{u}(\pi)]_{r=1} \qquad (46)$$

where $\tau_y(0)$ and $\tau_{xy}(0)$ are the singular parts of the stresses at $\theta = 0$ and $r = 1$, and $\dot{v}(\pi)$ and $\dot{u}(\pi)$ are the singular parts of the particle velocities evaluated at $\theta = \pi$ and $r = 1$. Substituting $\dot{u}(\pi) = (1/2)c(t)U(\pi)T(t)$, and $\dot{v}(\pi) = (1/2)c(t)V(\pi)T(t)$ it follows:

$$\gamma_0 = \frac{\pi}{4}[\tau_y(0)V(\pi) + \tau_{xy}(0)U(\pi)]_{r=1} T(t) \qquad (47)$$

Here $\gamma_0 = (1/2)F/c(t)$ = one half of the specific energy of crack extension. In some materials γ_0 may be nearly constant and nearly equal to the specific surface energy γ_F, while in other materials γ_0 may depend on $c(t)$, and may be much higher than γ_F.

To introduce appropriate normalizations it follows from equation (47) that if an eigenstate $X_i(\theta)$ yields for $G_{xy} = 1$ the value $\gamma_0 = \bar{\gamma}_0$, the eigenstate $kX_i(\theta)$ yields for $G_{xy} = 1$ the value $\gamma_0 = \bar{\gamma}_0 k^2$. Thus, to normalize an arbitrary eigenstate $X_i(\theta)$ as an eigenstate corresponding to $\gamma_0 = 1$ and $G_{xy} = 1$, the computer program was set up to multiply all computed X_i-values by the factor $k = (1/\bar{\gamma}_0)^{1/2}$. The values thus calculated have been plotted in Figs. 2–5. In order to obtain an eigenstate corresponding to given values of γ_0 and G_{xy}, the normalized X_i must be multiplied by $(\gamma_0/G_{xy})^{1/2}$, while all stresses computed from the normalized eigenstates must be multiplied by $(\gamma_0 G_{xy})^{1/2}$. Accordingly, the expessions $X_i(G_{xy}/\gamma_0)^{1/2}$ and $\tau_\theta/(\gamma_0 G_{xy})^{1/2}$, which represent nondimensional quantities, have been selected as the ordinates in Figs. 2–5.

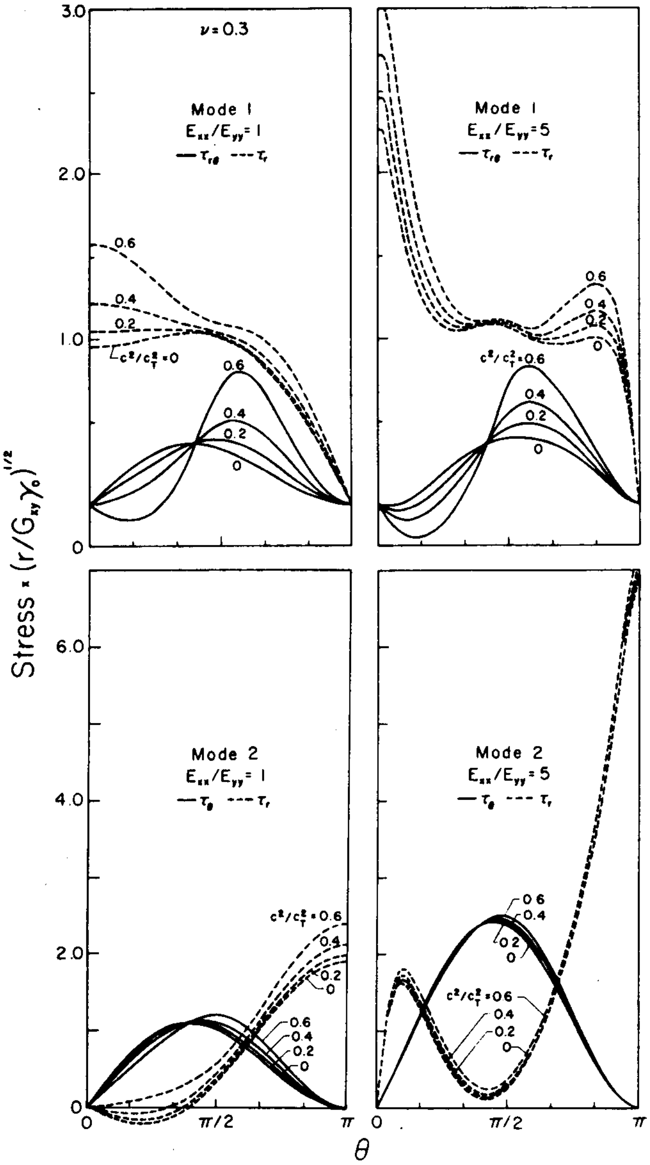

Fig. 4 Angular variation of stresses; the values of G_{yx}/E_{yy} and E_{xy}/E_{yy} equal those for an isotropic material of ν = 0.3

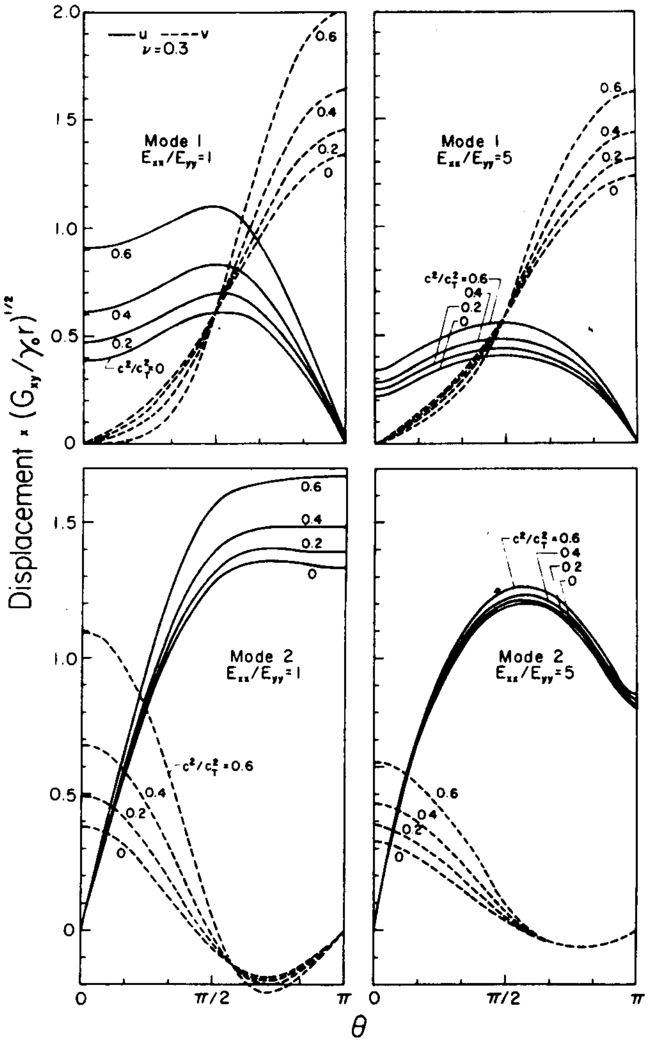

Fig. 5 Angular variation of displacement components; the values of G_{yx}/E_{yy} and E_{xy}/E_{yy} equal those for an isotropic material of ν = 0.3

Numerical Results and Discussion

Fig. 2 shows the dimensionless circumferential stress τ_θ versus the angle θ, for four values of c^2/c_T^2 in Mode I fracture of orthotropic materials. Computations were carried out for several values of E_{xx}/E_{yy}. For $E_{xx} > E_{yy}$ (or $E_{xx} < E_{yy}$) the values of G_{xy}/E_{yy} (or G_{xy}/E_{xx}) and E_{xy}/E_{yy} (or E_{xy}/E_{xx}) were chosen as those of an isotropic material, i.e., as $(0.5 - \nu)/(1 - \nu)$ and $\nu/(1 - \nu)$, respectively, where ν was selected as $\nu = 0.3$. The numerically computed curves for isotropic materials, which are labeled by $E_{xx}/E_{yy} = 1$, did not show any appreciable difference with analytical expressions from the section, "Analytical Approach."

Let us first consider a crack propagating in an isotropic material with Poisson's ratio $\nu = 0.3$. It is noted that the maximum value of the circumferential stress remains in the plane of crack propagation ($\theta = 0$) until c^2/c_T^2 reaches a value in between $c^2/c_T^2 = 0.4$ and $c^2/c_T^2 = 0.6$. As c^2/c_T^2 increases the maximum moves out of the plane of crack propagation. The influence of Poisson's ratio on this effect is also indicated in Fig. 2. The curves show that for smaller values of ν the maximum moves away from $\theta = 0$ at smaller values of the speed of crack propagation.

It appears that results for the elastodynamic near-tip fields for cracks propagating in orthotropic materials have so far not been available in the literature, except for the static case, which was discussed by Sih and Liebowitz, reference [12, p. 130]. When E_{xx}/E_{yy} is large enough, the maximum value of τ_θ may never be in the plane $\theta = 0$; even for $c^2/c_T^2 = 0$, as can be seen from Fig. 2. When E_{xx}/E_{xy} increases the shift of the maximum value of τ_θ from the plane of crack propagation is very pronounced, even at small values of c^2/c_T^2.

The dimensionless shear stress $\tau_{r\theta}$ is plotted in Fig. 3 for Mode II fracture. Although the general trends of the results are similar to those for the circumferential stress in Mode I fracture, the differences between the results for various values of c^2/c_T^2 are less pronounced. A noticeable variance with the Mode I case is the change of sign of the shear stress near $\theta = \pi/2$.

The influence of c^2/c_T^2 on various stress components for both Mode I and Mode II fracture is shown in Fig. 4. These curves also show some appreciable differences between the isotropic and the orthotropic cases.

Near-tip displacement fields are shown in Fig. 5. Information on the near-tip displacement fields is required for the formulation of a singular finite element in an elastodynamic finite-element analysis of the stress fields induced by a rapidly moving crack tip.

In this paper, the trajectories of crack propagation are taken as rather arbitrary for isotropic materials, and they are confined to planes of material symmetry for orthotropic materials. The trajectories that cracks will actually follow in the various fracture modes depend on the fracture criterion for a particular material. The results of this paper indicate, however, the crack propagation velocities at which the crack trajectories may depart from assumed ones. For example, if the crack trajectory is expected to follow the direction of the maximum circumferential stress, the results show the velocity at which the maximum circumferential stress-intensity factor shifts out of a smooth crack trajectory. A criterion of fracture at critical values of circumferential stress-intensity factors cannot be satisfied for the cases of Mode II fracture considered here, as is evident from Fig. 4, which shows that the maxima of τ_θ never are at $\theta = 0$. In general, fracture criteria involve, however, more complicated considerations. In this paper attention was, therefore, restricted to an investigation of the fields of stress and displacement for rapid crack propagation along certain rather general trajectories. The question whether or not, and under what circumstances, cracks will actually propagate along such trajectories falls outside the scope of this paper.

Acknowledgment

The work of one of the authors (J.D.A.) was carried out in the course of research sponsored by the National Science Foundation under Grant GK 26217 to Northwestern University.

References

1 Yoffe, E. H., "The Moving Griffith Crack," *Philosophical Magazine*, Vol. 42, Series 7, 1951, p. 739.

2 Craggs, J. W., "On the propagation of a Crack in an Elastic-Brittle Material," *Journal of the Mechanics and Physics of Solids* Vol. 8, 1960, p. 66.

3 Baker, B. R., "Dynamic Stresses Created by a Moving Crack," JOURNAL OF APPLIED MECHANICS, Vol. 29, TRANS. ASME, Vol. 84, Series E, 1962, p. 449.

4 Achenbach, J. D., "Dynamic Effects in Brittle Fracture," *Mechanics Today*, ed., Nemat-Nasser, S., Vol. 1, Pergamon Press, 1974, p. 1.

5 Knein, M., "Zur Theorie des Druckversuchs," *Abhandlungen aus dem aerodynamischen Institut an der T. H. Aachen*, Vol. 7, 1927, p. 62.

6 Williams, M. L., "Stress Singularities Resulting From Various Boundary Conditions in Angular Corners in Extension," JOURNAL OF APPLIED MECHANICS, Vol. 19, TRANS. ASME, Vol. 74, 1952, p. 526.

7 Cotterell, B., "On the Nature of Moving Cracks," JOURNAL OF APPLIED MECHANICS, Vol. 31, TRANS. ASME, Vol. 86, Series E, 1964, p. 12.

8 Rice, J. R., "Mathematical Analysis in the Mechanics of Fracture," *Fracture*, ed., Liebowitz, H., Academic Press, 1968, p. 191.

9 Freund, L. B., and Clifton, R., "On the Uniqueness of Plane Elastodynamic Solutions for Running Cracks," *Journal of Elasticity*, in press.

10 Nilsson, F., "A Note on the Stress Singularity at a Nonuniformly Moving Crack Tip," *Journal of Elasticity*, Vol. 4, 1974, p. 73.

11 Achenbach, J. D., *Wave Propagation in Elastic Solids*, North-Holland Publishing Co./American Elsevier, Amsterdam/New York, 1973, p. 58.

12 Sih, G. C., and Liebowitz, H., "Mathematical Theories of Brittle Fractures," *Fracture*, ed., Liebowitz, H., Academic Press, 1968, p. 96.

13 Bažant, Z. P., "Three-Dimensional Harmonic Functions Near Termination or Intersection of Gradient Singularity Lines: A General Numerical Method," *International Journal of Engineering Science*, Vol. 12, 1974, p. 221.

14 Bažant, Z. P., and Keer, L. M., "Singularities of Elastic Stresses and of Harmonic Functions at Conical Notches or Inclusions," *International Journal of Solids and Structures*, Vol. 10, 1974, pp. 957–964.

15 Freund, L. B., "Energy Flux Into the Tip of an Extending Crack in an Elastic Solid," *Journal of Elasticity*, Vol. 2, 1972, p. 341.